TECHNICAL MEMORANDUMS

NATIONAL ADVISORY COMMITTEE FOR AERONAUTICS

No. 502

ANALYSIS OF FLIGHT AND WIND-TUNNEL TESTS ON UDET AIRPLANES WITH REFERENCE TO SPINNING CHARACTERISTICS

By H. Herrmann

From Zeitschrift für Flugtechnik und Motorluftschiffahrt
January 14, 1929

Washington
March, 1929

NATIONAL ADVISORY COMMITTEE FOR AERONAUTICS.

TECHNICAL MEMORANDUM NO. 502.

ANALYSIS OF FLIGHT AND WIND-TUNNEL TESTS ON UDET AIRPLANES WITH REFERENCE TO SPINNING CHARACTERISTICS.*

(Low-wing Udet U 6, Udet U 7 "Kolibri," Udet U 12 "Flamingo.")

By H. Herrmann.

Introduction

During 1923-1925 many different types of light airplanes were made in Germany. For the analysis of the results attained, many comprehensive wind-tunnel tests were made in Göttingen at the suggestion of the writer with three different models constructed by him. The results were reported to the D. V. L. (German Institute for Aeronautic Research) of Berlin-Adlershof, which, in turn, commissioned the writer with their analysis.

The values were determined for the effectiveness of all the controls at various angles of attack. The autorotation was studied by subjecting the rotating model to an air blast. With the low-wing monoplane U 6 the aerodynamic longitudinal moment decreases suddenly at large angles of attack. The inertia forces then exceed the air forces and prevent escape from the spin. This actually occurred with this type. Recently a similar accident happened to another monoplane. The causes of the disastrous drop in the longitudinal moment

*"Auswertung von Flugversuchen und Windkanalmessungen an den Udet-Flugzeugen." From Zeitschrift für Flugtechnik und Motorluftschiffahrt, January 14, 1929, pp. 3-15.

have not yet been explained.

Symbols Used

F	m^2	Wing area including fuselage section and ailerons.
g	kgm/s^2	Acceleration due to gravity.
γ	kg/m^3	Air density.
v	m/s	Speed or velocity.
q	kg/m^2	Dynamic pressure $v^2/2g$.
t	m	Reference chord.
b	m	Span.
x	m	Abscissa of center of gravity.
y	m	Ordinate of center of gravity.
u	m/s	Peripheral velocity.
G	kg	Total weight.
W	kg	Drag.
S	kg	Lateral force.
c_a		Coefficient of lift, $c_a = \frac{G}{F} q$.
c_w		" " drag, $c_w = \frac{W}{F} q$.
c_s		" " lateral force, $c_s = \frac{S}{F} q$.
c_n		" " normal force, $c_n = c_a \cos\alpha - c_w \sin\alpha$.
c_t		" " tangential force, $c_t = c_w \cos\alpha - c_a \sin\alpha$.
M_H	mkg	Pitching moment due to air forces, positive when nose-heavy.
M_Q	mkg	Rolling moment due to air forces, positive when causing rotation to the right.

M_S	mkg	Lateral moment due to air forces, positive when causing a turn to the right.
M_K	mkg	Pitching moment due to the inertia forces, positive when nose-heavy.
		Pitching moment due to the gyroscopic moment of the propeller, positive when nose-heavy.
c_{mh}		Coefficient of pitching moment $\frac{M_H}{F}$ F t q.
c_{mq}		" " rolling " $\frac{M_Q}{F}$ t q.
c_{ms}		" " lateral " $\frac{M_S}{F}$ t q.

Axes through center of gravity and fixed in space:

x-axis in the direction of flight;

y-axis perpendicular to the direction of flight;

z-axis parallel to the direction of flight.

Axes through center of gravity and moving with the airplane:

x', longitudinal axis;

y', vertical axis;

z', lateral axis.

J_x, J_y, J_z mkg/s², inertia moments about the 3 axes.

ω_x, ω_y, ω_z l/s, angular velocities about the 3 axes.

α	Angle of attack.
φ	Angle of flight path.
μ	Angle of roll.
τ	Lateral angle, positive when airplane turns to left.
β_H	Elevator angle, positive when causing nose-heaviness.

β_Q Elevator angle, positive when causing right roll.

β_S Rudder angle, positive toward the right.

1. Historical Sketch

The U 6 was built in January-February, 1923, and was flown in May. It surpassed the other airplanes of that time. It was purposely made slightly nose-heavy and was balanced by 5 kg (11 lb.) of ballast in the tail.

Type		U 6	U 7	U 12
Year built		1923	1924	1925
Span	m	9.8	10	10
Distance of elevator from center of gravity	m	3.7	3.5	4.3
Reference chord	m	1.50	1.50	1.32
Wing area including ailerons	m^2	12	12.5	24
Aileron area	m^2	1.2	1.2	1.4
Stabilizer area	m^2	1.8	1.8	1.5
Elevator "	m^2	0.8	0.8	0.8 (1.05)*
Fin "	m^2	0.25	0.25	0.45 (0.70)*
Rudder "	m^2	0.30	0.30	0.54 (1.00)*
Dead load (weight empty)	kg	330	165	500
Useful load	"	220	85	300
Total "	"	550	250	800

*The parentheses refer to spinning tests. The other numbers refer to wind-tunnel tests.

Engine power	HP.	55	18	80
Maximum speed	km/h	145	95	140
Climbing speed (air density 1 kg/m³)	m/s	ca. 1.0	0.6	1.2
Maximum lift coefficient attained		–	–	–
Take-off run	m	200	100-200	130
Landing run	m	125	80	150
Inertia moment about vertical axis,	mkg/s²	90	77	234
Inertia moment about longitudinal axis	mkg/s²	60	53	184
Inertia moment about lateral axis	mkg/s²	50	38.5	150
Inertia moment of propeller	mkg/s²	0.211	0.079	0.174
Abscissa of center of gravity	m	0.74	0.64	0.75
Ordinate of center of gravity	m	+0.30	-0.45	-0.93

Flight characteristics.- Longitudinal stability with and without gas. Lateral stability of curves up to 30°. Like high effectiveness of all three controls. Uniform almost zero pressure on all controls. Very sensitive in flight. Looping and rolling showed that the elevator was very small for such stunts.

Once pilot D. forced the airplane into a spin. It spun very slowly at a large angle of attack. The engine remained still, and the pilot could not get out of the spin. He was very familiar with spinning, had good nerves and presence of mind and escaped uninjured on crashing in the woods. He had done all that was humanly possible to get out of the spin and reported that all the controls were pressureless and ineffective.

The U 7 ("Kolibri") was built in November, 1923; remained idle three months for lack of an engine; was first flown in June, 1924, and won three first prizes the same year in the Rhön contests. The rudder had to be enlarged. It could not be considered perfect. It was intended for training purposes, but failed as regards the engine question. Two accidents, due to stalled flight at altitudes of 20-30 m (65-100 ft.) by incompetent pilots, could not be attributed to the characteristics of the airplane.

The U 12 ("Flamingo") was built in December, 1924 - February, 1925, and was first flown in March. It was found to be 5 cm (2 in.) tail-heavy as compared with the design. Since it was first used chiefly for stunt flying, no complaint was made, because a slight tail-heaviness facilitated looping and rolling.

The first sample did not exhibit the perfection which subsequently led to its general adoption. Its easy transition into and out of turns, combined with good lateral stability and controllability at large angles of attack, distinguished this type from the others of that time.

The elevator was first enlarged. The inner contour was then cut away, in order to produce a pressure equal to that on the ailerons. This proved successful. For the same reason the rudder was likewise enlarged toward the rear. Thus it was brought about that all the controls produced the same angular acceleration for the same pressure and motion of the hand or foot. The sensitivity to gusts was also the same about all three axes.

The following incident then occurred, which affected the whole development. Von K., a new pupil who had never been in a spin before, came out of a flat spin into a close spiral, apparently without recognizing it soon enough and high enough, and struck the side of a house. The airplane had an enlarged elevator and rudder.

Up to that time no spinning had been tried with that type. Systematic spinning tests were made with it in November, 1925. Two rudders were used, one of them being enlarged backward and the other upward. Von Schönebeck was the pilot. The report reads:

"The tests yielded perfectly normal spinning curves up to five rotations and 350 m (1150 ft.) loss in altitude. With the aid of a triple recording device, there were measured the loss in altitude, the rotation time and the number of rotations during the whole spin. The radius was estimated, partly from the ground and partly from another airplane. The results were as follows.

Spin of the U 12

Number of the flight	Number of the spin	Altitude loss in m	Time per rotation	Number of rotations	Approximate speed of descent km/h
1	1	185	-	-	-
	2	160	3.5	2	82
	3	160	4.0	2	72
	4	204	2.5	$1\frac{1}{2}$	(195)
2	1	182	3.0	2-3/4	80
	2	285	2.5	4-1/2	143
	3	355	-	4	-

"The altitude loss was calculated with the aid of the Jordan altitude formula:

$$h = 16000 \, \frac{B - B_1}{B + B_1}, \; (1 - 0.004 \, t_m),$$

in which B denotes the barometric height at the end of the spin; B_1, the barometric height at the beginning of the spin; t_m, the mean temperature of the air stratum, which was put at -10°C (14°F). The values plainly show that (in comparison with English measurements) the spinning curves were perfectly normal. The radius of the flight path was estimated at 8-10 m (26-30 ft.).

"The spin was entered from a steep 'corkscrew' with full aileron and rudder deflection in the same direction and with the elevator up. The transition from the spiral into the spin was effected by a sudden jerk. The spin was uniform until the steering controls were released, when there was a gradual transition to normal flight. This usually required about 1.5 rotations.

"The enlarged rudder required 2 to 3 rotations before the requisite angular velocity for spinning was attained. The recovery from the spin was accomplished in about the same manner for both rudder sizes.

"Stalling in straight flight caused pancaking while stalling in a turn, without a very high angular speed, caused sideslipping.

"It seems advisable to use the enlarged fin and rudder because they tend strongly to prevent the transition into a spin."

It was therefore decided to use only the large fin and rudder. Subsequent tests made it seem advisable to enlarge the fin still further. These measures increased the tail-heaviness. The writer made flights with ballast in front of the center of gravity. These flights showed the best location for the center of gravity to be 5 cm (2 in.) in front of the location calculated from monoplane tests. The next series was then made with a correspondingly longer fuselage and advanced landing gear.

Two other tests led to no further structural changes. Once the wing contour was made rectangular in order to cheapen its production. The result was a lessened aileron efficiency and an increased pressure on the ailerons. There was no possibility of rolling. The dihedral was then eliminated with a much poorer control while going into and out of turns. Experience also showed that the elimination of the one degree of washout had an unfavorable effect on curvilinear flight. Lastly, the gear ratio of the control stick to the ailerons was raised, thus equalizing again the pressure and effectiveness of all the controls.

Characteristics of Production Airplanes

Characteristic	Means and cause
Equalization of pressure and effectiveness. Good transition into and out of turns.	Flight tests, changes in the controls. 3° dihedral, elliptical lift distribution crosswise to the flight direction obtained by 1° washout and wing plan form.
Ability to land easily.	No separation of flow at large angles and good effectiveness of all controls. Correct location of landing gear.
No loss of control in stalled flight, lateral stability at large angles of attack.	Elevator sufficiently effective to overcome the wing moment at large angles. Apparently no diminution of the lift coefficient at large angles. Wing-plan form.
Ability to do all kinds of stunt flying.	Control effectiveness.

Surfaces of the four types: varnished plywood fuselages and fins; fabric-covered wings, stabilizers, elevators and rudders. The wings of the U 6 and U 7 had leading edges of plywood. The wings of the U 12 had auxiliary ribs.

2. Wind-Tunnel Tests

Models with landing gears were made corresponding to Figures 1-3. The wings of the biplane were connected by thin streamlined struts, whose drags were not determined separately. The test results were not suitable for efficiency calculations.

Reference Quantities

The reference quantity for all forces and moments is the wing, including the central section.

The reference chord for all moments is the maximum chord near the fuselage.

The reference axis for the longitudinal or pitching moment is the lateral axis, fixed both with respect to the flight path and with respect to the airplane itself, passing through the foremost point of the chord in the middle of the wing (the upper wing of a biplane).

The reference axis for the rolling moment is the axis fixed with respect to the flight path and passing through the foremost point of the wing chord in the plane of symmetry parallel to the direction of the wind.

The reference axis for the turning moment is the axis fixed with respect to the flight path and passing through the foremost point of the chord in the center of the wing perpendicular to the direction of the wind.

A n g l e s

The angle of attack is the angle between the line of thrust and the direction of the air flow. On the U 12 it is the angle between the chord of the upper wing and the direction of the air flow.

The angle of yaw is the angle between the longitudinal axis of the airplane and the flight path.

The lateral angle is determined from the angle of attack and the angle of yaw.

There were measured:

1. With the three-component balance, the lift, drag and pitching moment at angles of -30° to $+40^\circ$ for all three models with rudder neutral.

2. With the six-component balance, the effect of a deflection of 20° of the elevator, rudder and ailerons for all three models throughout the whole range of angles of attack. For testing the ailerons and rudder at negative angles of attack, the elevator deflection was plus 20°. For positive angles of attack, the elevator deflection was negative, corresponding to conditions in practice. The elevator was set at zero for medium angles of attack.

3. Only on the U 12, the effect of angles of yaw of 15 and 30 degrees on all forces measured under heading 2.

4. For all three models, rotation produced by the deflection of the ailerons and autorotation about an axis passing through the center of gravity.

Arrangement of Apparatus

A shaft, passing through the point in the model which corresponded to the center of gravity of the full-sized airplane, was rotatably mounted on the bearings A and B (Figs. 4 and 5). The model itself was, in turn, made rotatable longitudinally about the center of gravity, in order to obtain the different angles of attack. An adjustable counterweight G was added, in order to obtain a uniform angular velocity.

The Experiment

The revolution speed of the model was determined at various angles of attack α, aileron deflections β_q (from 0 to 20°) and wind velocities v, the maximum value of which was determined by the strength of the model. For angles of attack below 16° the rudder had to be removed, because it hit the shaft. Control readings at large angles of attack, without the tail members, showed no measurable differences.

The model was sometimes set in motion at $\beta_q = 0$, and the spinning direction determined. No special tendency to spin in either direction, or to begin to spin without starting, was noticed with any model, though it should be noted that there was some friction in the bearings. The starting was also attempted, though always unsuccessfully, at $\beta_q = 10°$ and 20° with large angles of attack outside the spinning range. Spinning in the opposite direction to that produced by the ailerons was effected only twice (with the U 6 and U 12) in spite of repeated attempts. Two positions of spinning equilibrium were found at large angles of attack. On gradually increasing the wind velocity from zero, the lower position of equilibrium was obtained, which then quite suddenly went over into the upper position of equilibrium at high wind velocities. The latter position then persisted, even when the wind velocity was reduced. The revolution speed was determined as nearly as possible for both positions, but it could not always be found accurately, on account of the instability at high velocities and on account of the friction of the bearings at low velocities.

A n a l y s i s

The peripheral velocity $u = \omega \frac{b}{2}$ was determined from the measured revolution speed.

M o d e l s

a) U 6.- Both directions of turning were tried in order to compare the uniformity of the left and right turn. The slight differences were probably due to the lack of perfect symmetry of the model. Smaller angles of attack than the ones measured could not be obtained. At $\alpha = 24.8^{\circ}$ it was found possible to make the model spin contrary to the turning direction determined by the deflection of the ailerons.

b) U 7.- The trailing edge of the middle portion of the wing had to be cut away. When α was smaller than 11°, a portion of the fuselage nose also had to be removed. Here also the control points, at greater angles of attack without the fuselage nose, gave no measurable differences.

c) U 12.- The trailing edge of the middle portion of the upper wing had to be cut away. At $\alpha = 23.8^\circ$ and $\beta_q = 10^\circ$ it was found possible to make the model spin contrary to the turning direction determined by the deflection of the ailerons.

The experimental results are shown in Figures 15-17.

3. Inertia Moments

Before definitely determining the spinning conditions, we must determine the moments produced by the inertia forces. We do this first for the angular velocity $\omega = 1$. In determining the actual inertia moments we then have only to introduce the actual angular velocity. Contrary to the air forces, they must be referred to the axes moving with the airplane. For their calculation we use the inertia ellipsoid of the airplane. Its axes form angles of 1 to 3 degrees with the axes of the airplane. The centrifugal force thus produced is disregarded.

Before we begin with the calculation, we will first determine to what variables we will restrict ourselves, since relations too troublesome for practical purposes would otherwise occur. Since the gyroscopic moments here depend on rotation in space and not about the flight path, we must take into account both the angle of attack and the slope of the flight path. If we imagine the steep spiral developed, we then have an inclined plane at an angle equal to that of the flight-path angle, on which the airplane descends at a large angle of attack. Thereby a small lateral angle τ, or a small angle of roll μ, greatly affects the air forces and air-force moments, but only slightly affects the inertia moments. If the inclined plane is again coiled into a spiral, the inner wing tip acquires a greater angle of attack and consequently a greater drag.

A moment is thus produced about the vertical axis. This is opposed by a second moment, in that the tail in the spiral no longer receives the wind symmetrically but laterally from without. The magnitude of these moments is not known, but must be quite large. From experience, it is known, however, that the lateral and rolling angles occurring in practice are quite small. The gyroscopic moments about the vertical and longitudinal axes are thus eliminated. Consideration of the lateral angle slightly reduces the inertia moments. The gyroscopic moment about the remaining axis of roll, during steady motion, is

$$M_K = (J_x - J_y)\ \omega_x\ \omega_y.$$

The components of the angular velocity are

$$\omega_x = \omega \sin (\varphi - \alpha) \quad \text{and} \quad \omega_y = \cos (\varphi - \alpha).$$

The introduction of these values yields the simple formula

$$M_K = (J_x - J_y)\ \omega^2 \tfrac{1}{2} \sin 2\ (\varphi - \alpha).$$

With the aid of the values mentioned at the beginning, the calculation is now a simple matter. We assume the flight-path angle to be 70°, which is a conservative mean value. Figure 18 shows the result. At large angles the curve falls off.

If we now compare the inertia forces for $\omega = 1$ of the low-wing monoplane with that of the high-wing, we find a smaller gyroscopic moment for the former. The gyroscopic moment of the biplane is greater, corresponding to the greater weight, and (taking this fact into account) not fundamentally different. The high-wing monoplane really has the greatest inertia forces in proportion to its small weight. For flight conditions the square of the angular velocity is more important than the individual structural type, when the latter does not fundamentally alter the air forces. Wee will see later, however, that the contrary case sometimes occurs.

Gyroscopic Moments

The gyroscopic moment of the propeller, however, is not proportional, as hitherto, to the second power of the angular velocity, but only to the first power. The moment about the lateral axis of the propeller, with the inertia moment J_L and the angular velocity ω_L due to rotation about the vertical axis, is

$$M_g = J_L \, \omega_L \, \omega \sin (\varphi - \alpha),$$

Figure 18 shows the calculation. It cannot be compared, however, with the lower curves, since the gyroscopic forces increase with the first power and the other inertia forces increase with the second power of the angular velocity. They are responsible for the difference between right and left spins. They become important only on the installation of an engine with a very large propeller on a small airplane with very great wing loading. Their inertia moment increases with the fifth power of the diameter. A Reed metal propeller has twice the weight and twice the inertia moment of a metal-tipped wood propeller. An untipped wood propeller has a still smaller weight and inertia moment. This difference may be decisive for single-seat pursuit and racing airplanes. The direction of rotation then assumes importance.

Propeller	Airplane	Moment	
Turning to the right	Right turn Right spin	Nose-heavy " "	Harder Easier
	Left turn Left spin	Tail-heavy " "	Easier Dangerous
Turning to the left	Left turn Left spin	Nose-heavy " "	Harder Easier
	Right turn Right spin	Tail-heavy " "	Easier Dangerous

4. Spinning

We turn next to the interesting problem of comparing the inertia forces in spinning with the aerodynamic longitudinal or pitching moment. We take the pitching moment (Figs. 19-21) from the Göttingen measurements for the position of the center of gravity. We determine the angular velocities from the results of the autorotation tests as shown in Figures 15-17. Thereby the following numbers represent the weight and velocity

$$1. \quad U\ 6)\ G = 450\ kg, \quad v = 4\sqrt{\frac{G}{F\ 1.1}} = 23.3\ m/s$$

This corresponds to the condition and to the inertia forces in diving.

$$2. \quad U\ 7)\ G = 300\ kg, \quad v = 4\sqrt{\frac{G}{F\ 1.2}} = 17.9\ m/s$$

This corresponds to the condition for normal flight.

$$3. \quad U\ 12)\ G = 670\ kg, \quad v = 4\sqrt{\frac{G}{F\ 1.1}} = 20.1\ m/s.$$

This corresponds to the spinning tests and inertia forces.

From the resulting angular velocities we find the inertia forces. They are plotted in Figures 19-21 and represent the following phenomena.

<u>a) U 6</u>.- The airplane got into a spin only once and failed to come out of it. At zero aileron deflection, the inertia moments equal the pitching moment without rotation. From English calculations and experiments we know that through rotation the pitching moment of the wing decreases at large angles of attack. If, in the present case, the wing moment be regarded as excessive, its smallness is the cause of the inability to come out of the spin. The inertia forces are rather great, due to the high peripheral velocity. The abnormality, however, is not the magnitude of the inertia forces, but the smallness of the longitu-

dinal or pitching moment. The already high angular velocity for the aileron deflection $\beta_q = 0$ is still further increased, in comparison with the other types, by the high-wing loading.

b) U 7.- This airplane went into a spin only once. It did this at an altitude of only 30 m (about 100 ft.) and immediately struck the ground. At a higher altitude it should have been able to spin without accident. Here also it is noticeable that the longitudinal moment decreases at large angles of attack.

c) U 12.- Many pupils have learned to spin with this type. The flight results are fully confirmed by calculation. At full rudder deflection, the inertia forces exceed the aerodynamic longitudinal moment and establish a position of equilibrium at 34 to 40 degrees with the elevator deflected upward. With all the controls deflected halfway, both the angular velocity and the inertia force decrease with a simultaneous increase in the nose-heavy longitudinal moment. The accident which occurred was due to the inexperience of the pupil.

d) The effect of the propeller is shown by the two lighter curves. It is tail-heavy or nose-heavy according to the direction of rotation.

5. Conclusion

The fall in the longitudinal moment of the U 6 has not been explained. Guesses are useless without proof. In this connection further wind-tunnel tests must be made. It will also be well to test the U 6 and U 7 in a lateral wind and also to exchange the wings of these two types. We can thus determine the difference between the high-wing and low-wing monoplane. The transition into and out of a turn is almost always combined with a lateral motion, whose great rolling moment is evident in the case of the U 12.

These considerations did not determine the real effective moment about the vertical and lateral axes, for which the lateral force, with its lever arm as the reference quantity, must be considered. From this we can determine the initial angular velocity produced by a 20° deflection of the ailerons or rudder. This is of value, however, only in tests with a lateral wind and exchanged wings.

Translation by Dwight M. Miner,
National Advisory Committee
for Aeronautics.

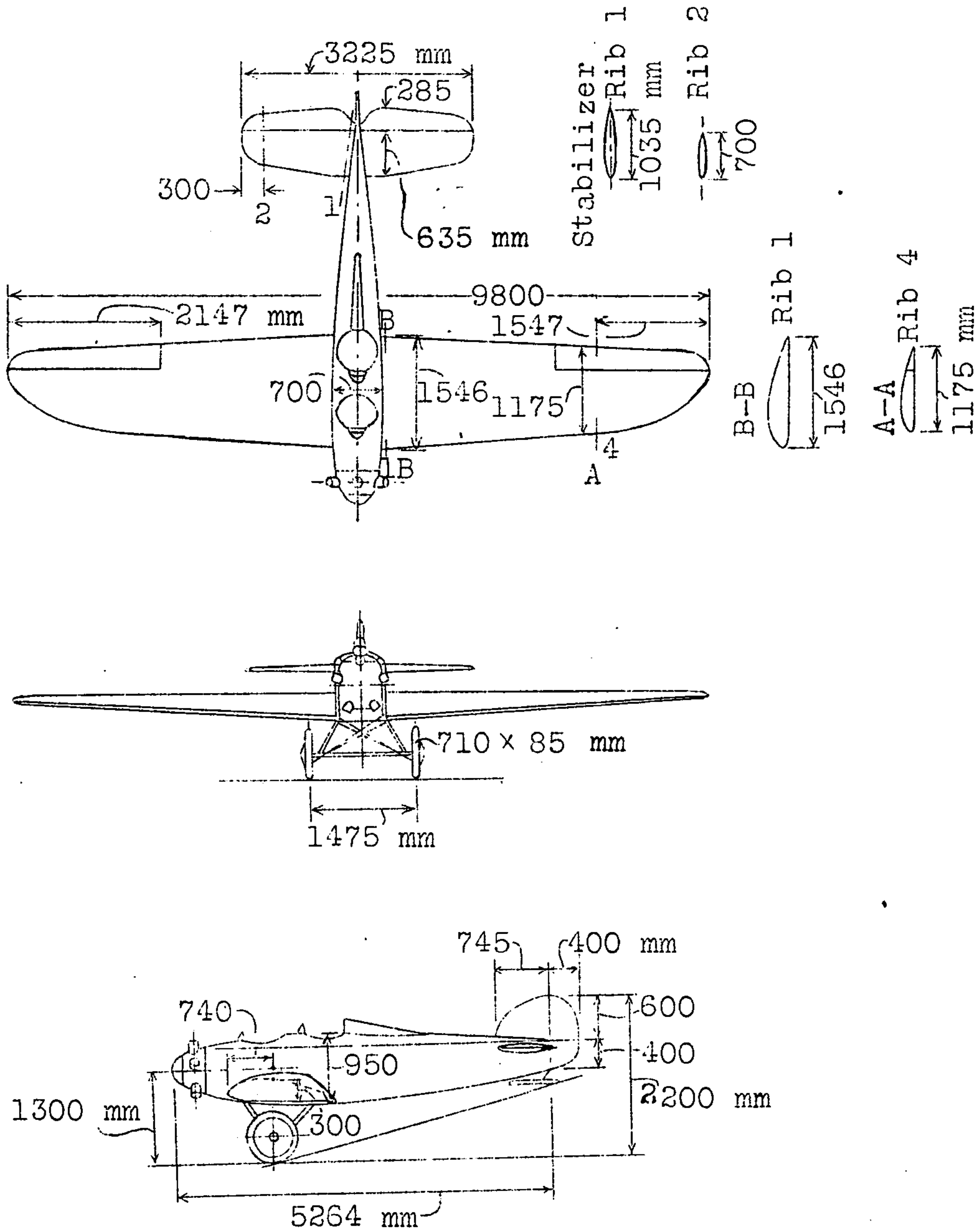

Fig.1 U6. Low wing monoplane.60 HP Siemens.2 seats.

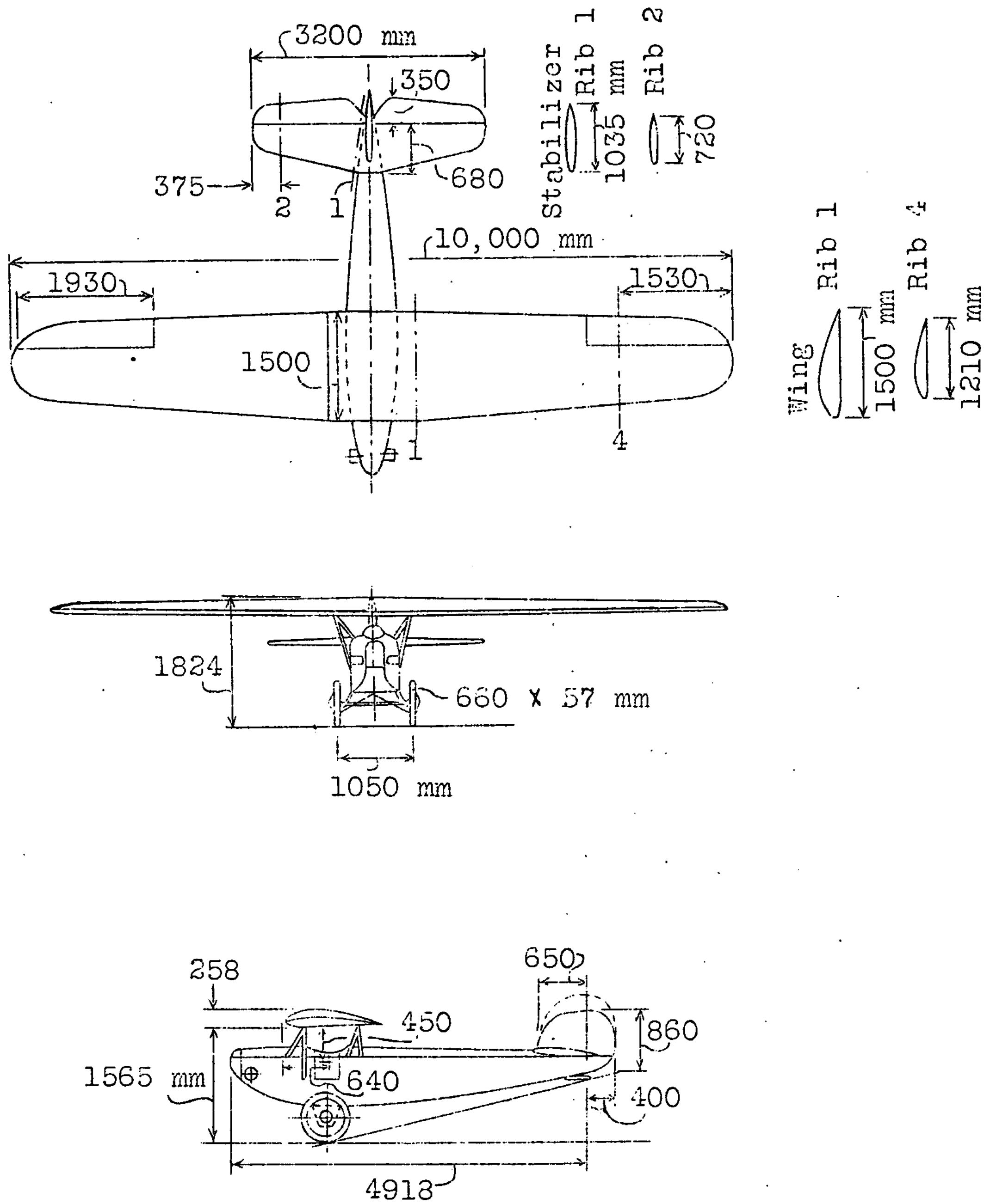

Fig.2 U7.Kolibri high wing airplane.20 HP engine.1seat. The change in position of center of gravity due to the enlarging and the fitting of a different (Siemens) engine made necessary an entirely different type of construction.The vertical fin and rudder used on the wind tunnel model are shown in dotted lines.

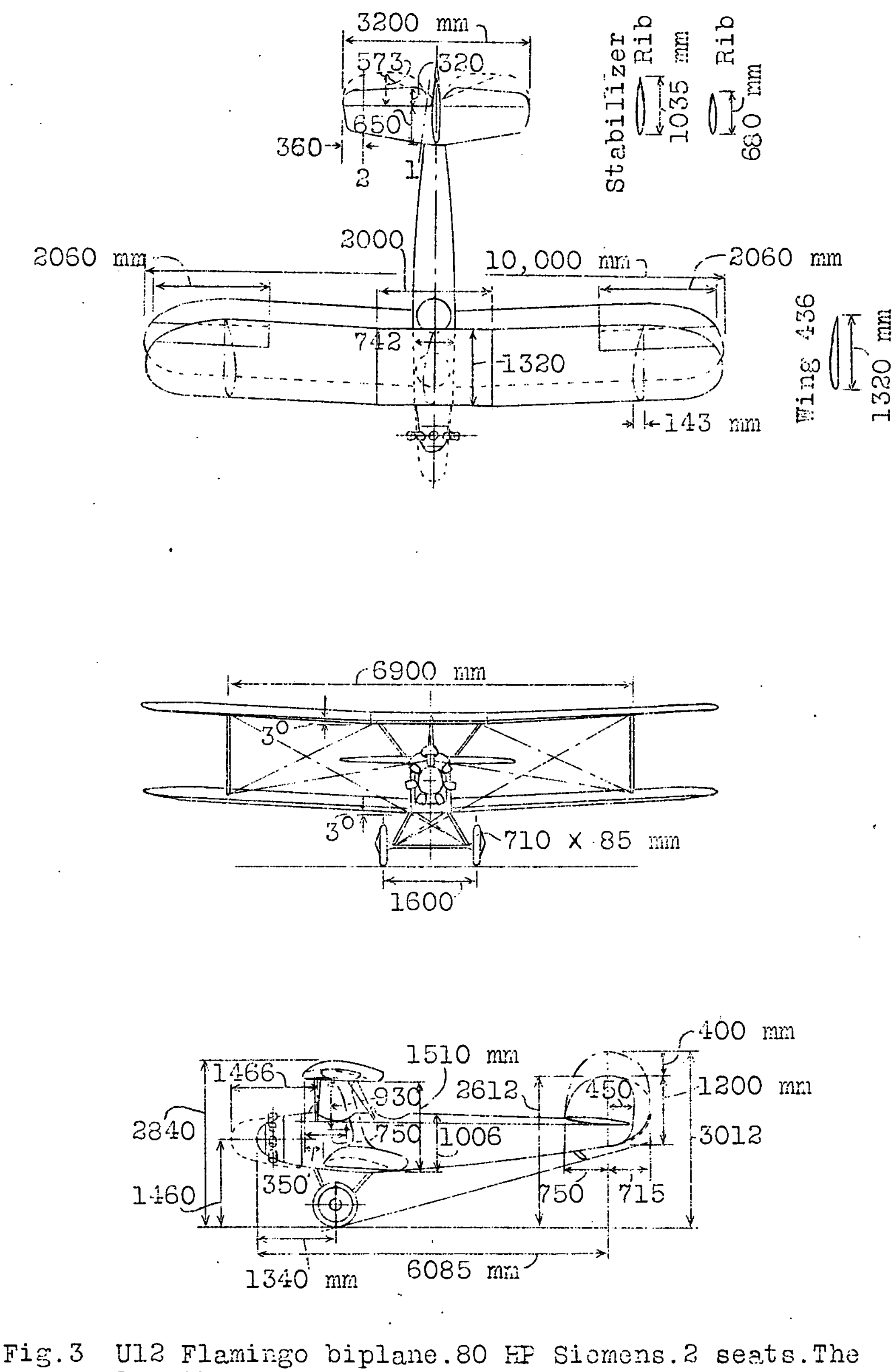

Fig.3 U12 Flamingo biplane.80 HP Siemens.2 seats.The lengthened fuselage and enlarged vertical fins and rudders used on the wind tunnel model are shown in dotted lines.

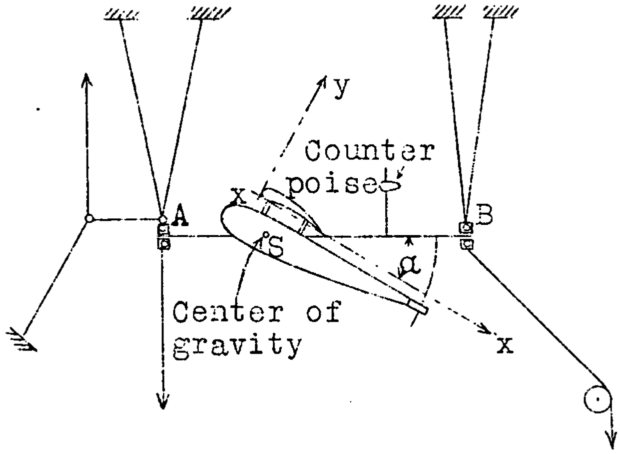

Fig.4 Installation for spinning test
in wind tunnel.

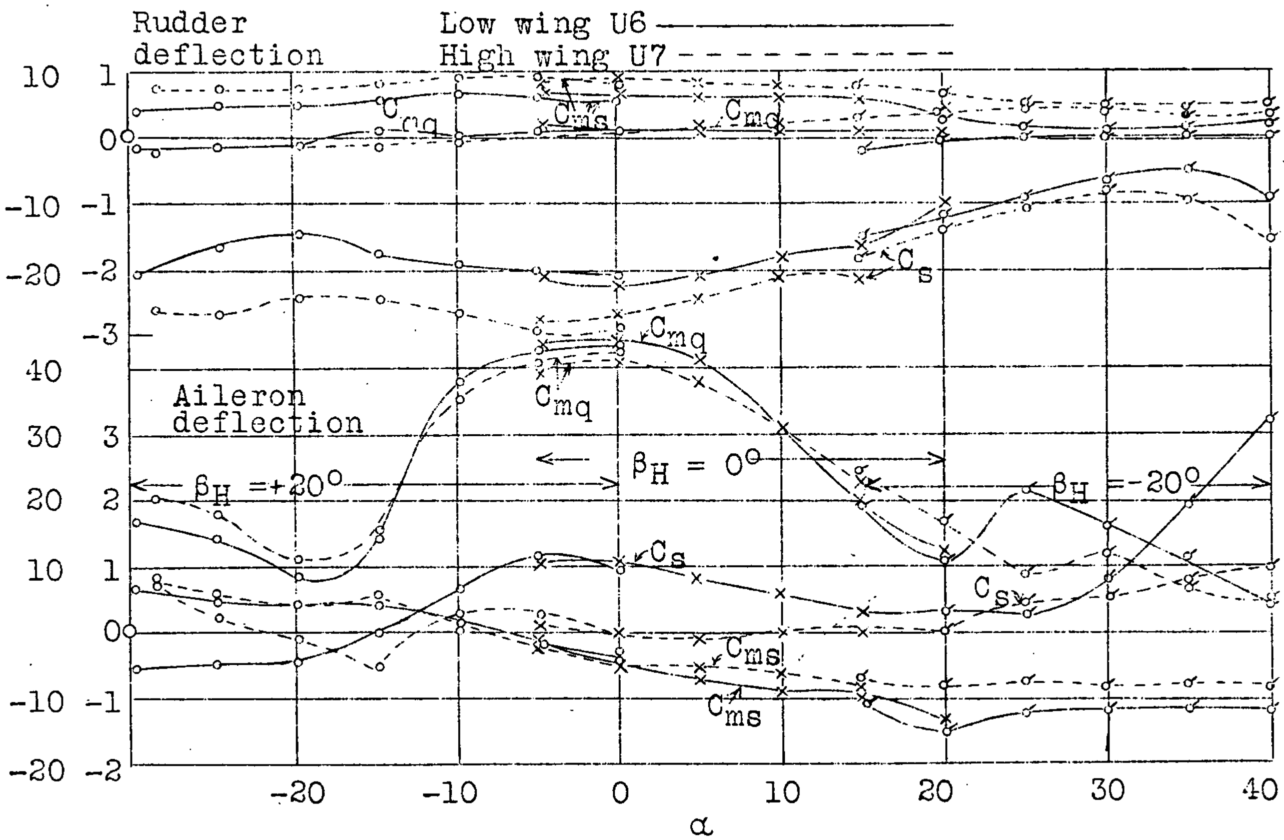

Fig.12 Effectiveness of ailerons and rudders on U6 and U7. The rudder forces and moments are greater on the high wing monoplane. Between 10° and 22° angle of attack the ailerons of U7 are superior because they produce larger rolling moments and smaller yawing moments, The smaller yawing moments are associated with the smaller increases in drag shown on the U7 polars and require smaller rudder movements to counter act them. The poor effectiveness of the rudder found in flight tests can be attributed to the lack of dihedral.

NOTE.- Subsequent to completion of report, legends of Figures 5, 6, 7, and 8 have been corrected to read as follows:

Fig. 5. Wind tunnel arrangement for spinning tests.

Fig. 6. U 6 polars.
Note the great increase in drag for control movements of 20° and the course of the moment curve at large angles of attack.

Fig. 7. U 7 polars.
Note the great increase in drag for control movements of 20°. The increase in drag due to movement of the ailerons is less with this plan form of wing than for the U 6. The ailerons are the same size. Note the course of pitching moment at large angles of attack.

Fig. 8. U 12 polars.
Note the great increase in drag for control movements of 20°. The increase in drag due to the ailerons is similar to that on U 7. The pitching moment no longer decreases with increasing angle of attack. This is the principal and most important difference as compared with the monoplanes.

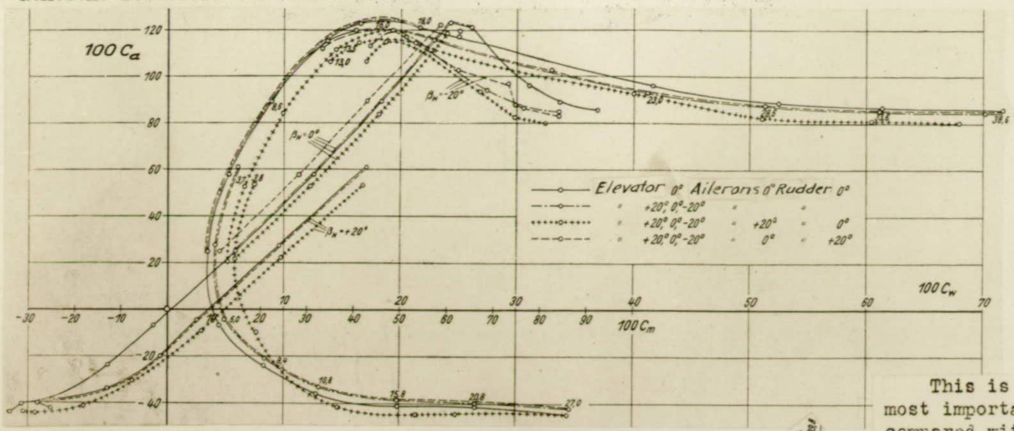

Fig.8 Udet U12 biplane polars. The great drag increase for deflections of 20° is shown. The drag increase of the ailerons is similar to that of the U7. The longitudinal moment no longer decreases with increasing angle of attack.

This is the principal and most important difference as compared with the monoplanes.

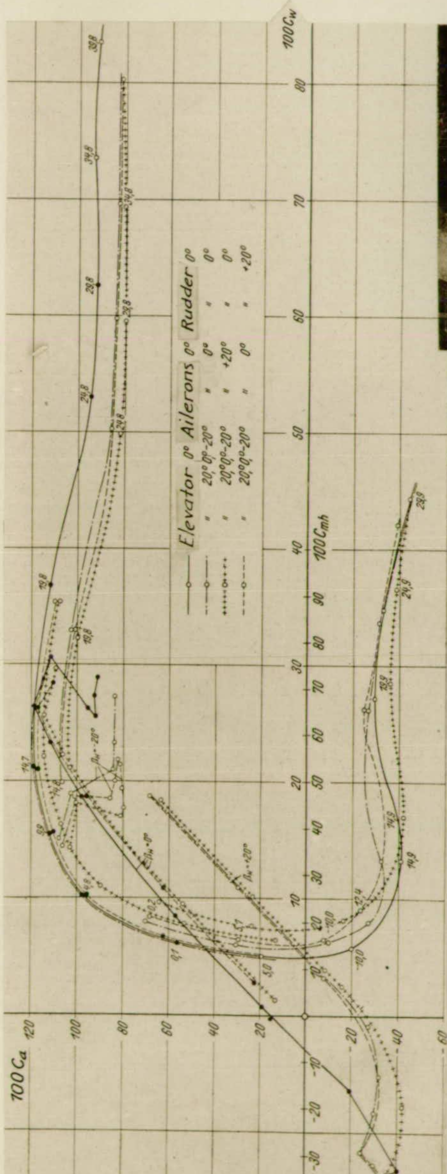

Fig.6 Low-wing Udet N6. Elevator 0° Rudder 0° U6 polars. The great drag increase for deflections of 20° is shown. Note the course of the moment curve at large angles of attack.

Fig.5 Wind tunnel installation for spinning test.

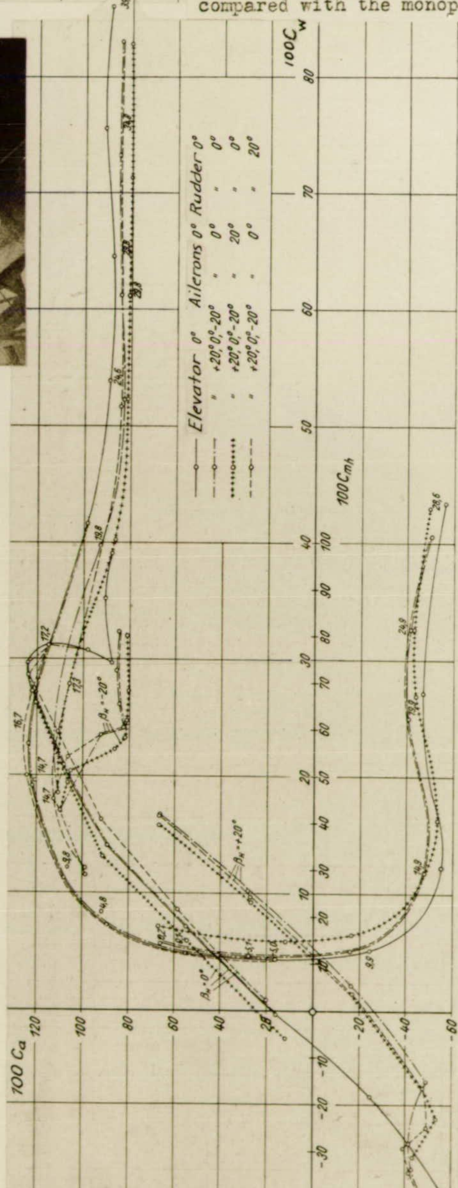

Fig.7 High-wing Udet U7. U7 polars. The great drag increase for deflections of 20° is shown. The drag increase of the ailerons is less than for the N.6. The size of the ailerons is the same. Note the course of the longitudinal moment at large angles of attack.

9429 A.S.

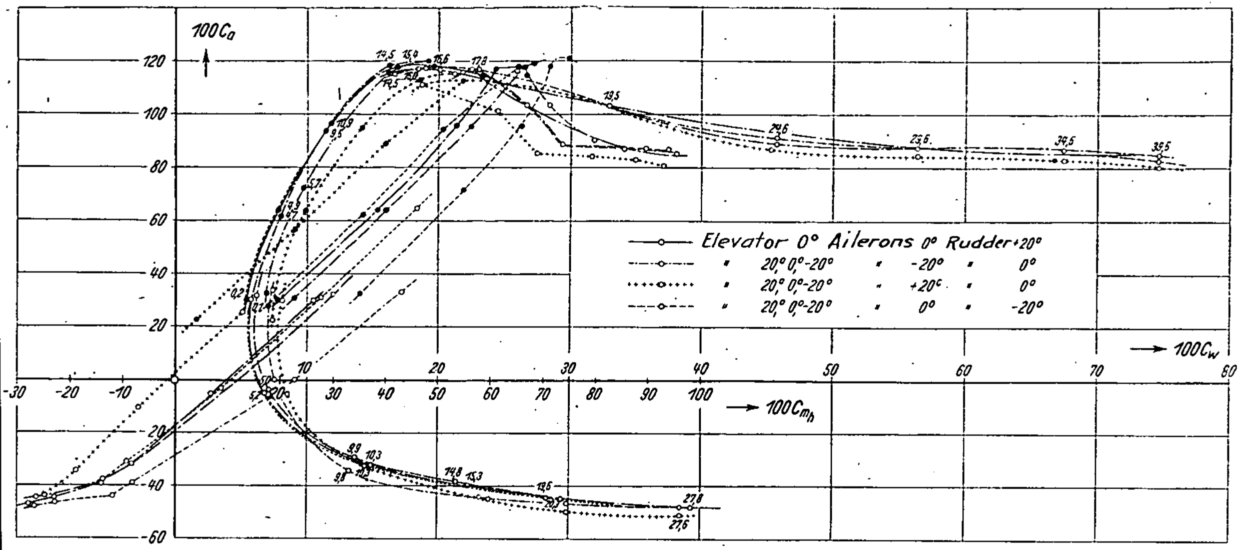

Fig.9 Udet biplane U12. U12 polars with 15° side wind. All the drags are greater.

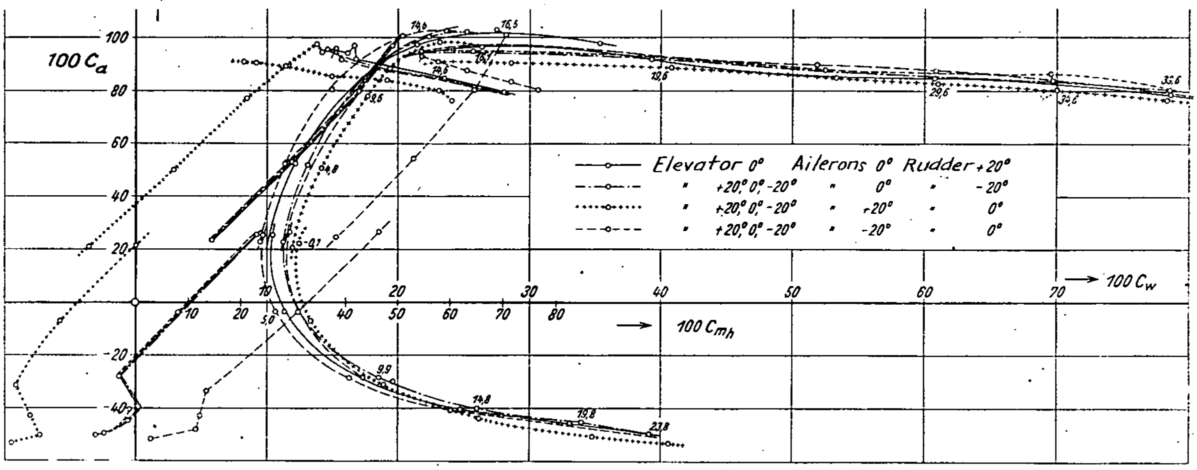

Fig.10 Udet biplane U12. U12 polars with 30° side wind. All drags are much greater.

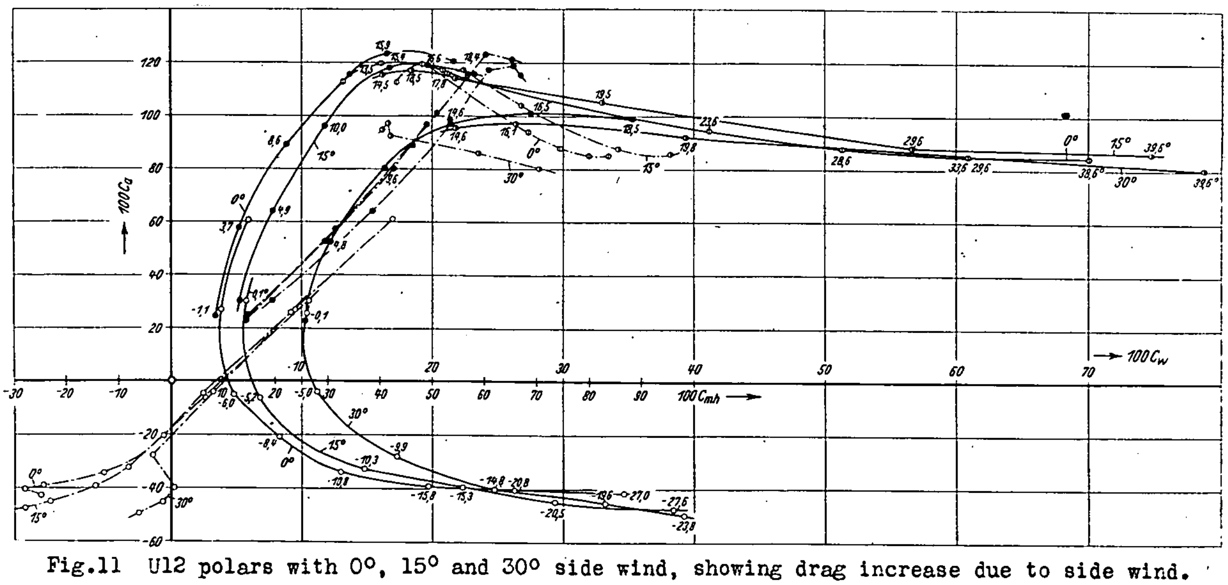

Fig.11 U12 polars with 0°, 15° and 30° side wind, showing drag increase due to side wind.

9430 A.S.

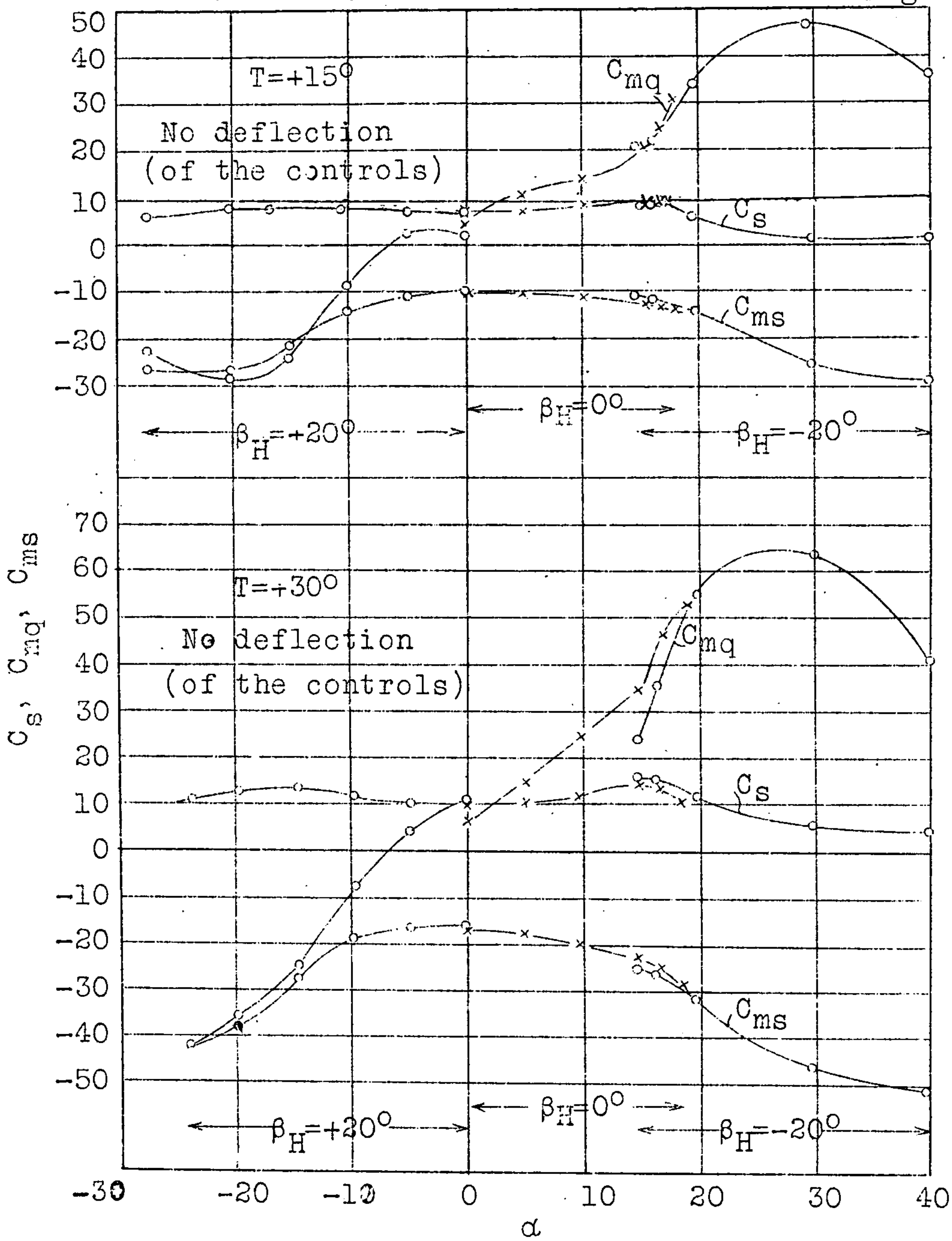

Fig.13 Effectivness of rudder and ailerons of the U12"Flamingo" with T = 0°,15° and 30° yaw. A yaw without movement of the ailerons gives a rolling moment which is twice as great as that produced by 20° movement of the ailerons at zero yaw. These values are affected only slightly by a 20° movement of the rudder, whose effectiveness increases with increasing angle of yaw. The effectiveness of the ailerons is increased by yaw.

Experience shows that to execute a roll first obtain excess power then give full rudder with bank,as senn as a heavy stick force is felt,indicating a large angle of yaw,give full aileron. The rudder used in flight tests was larger.

Fig.13 (continued on next two pages) a

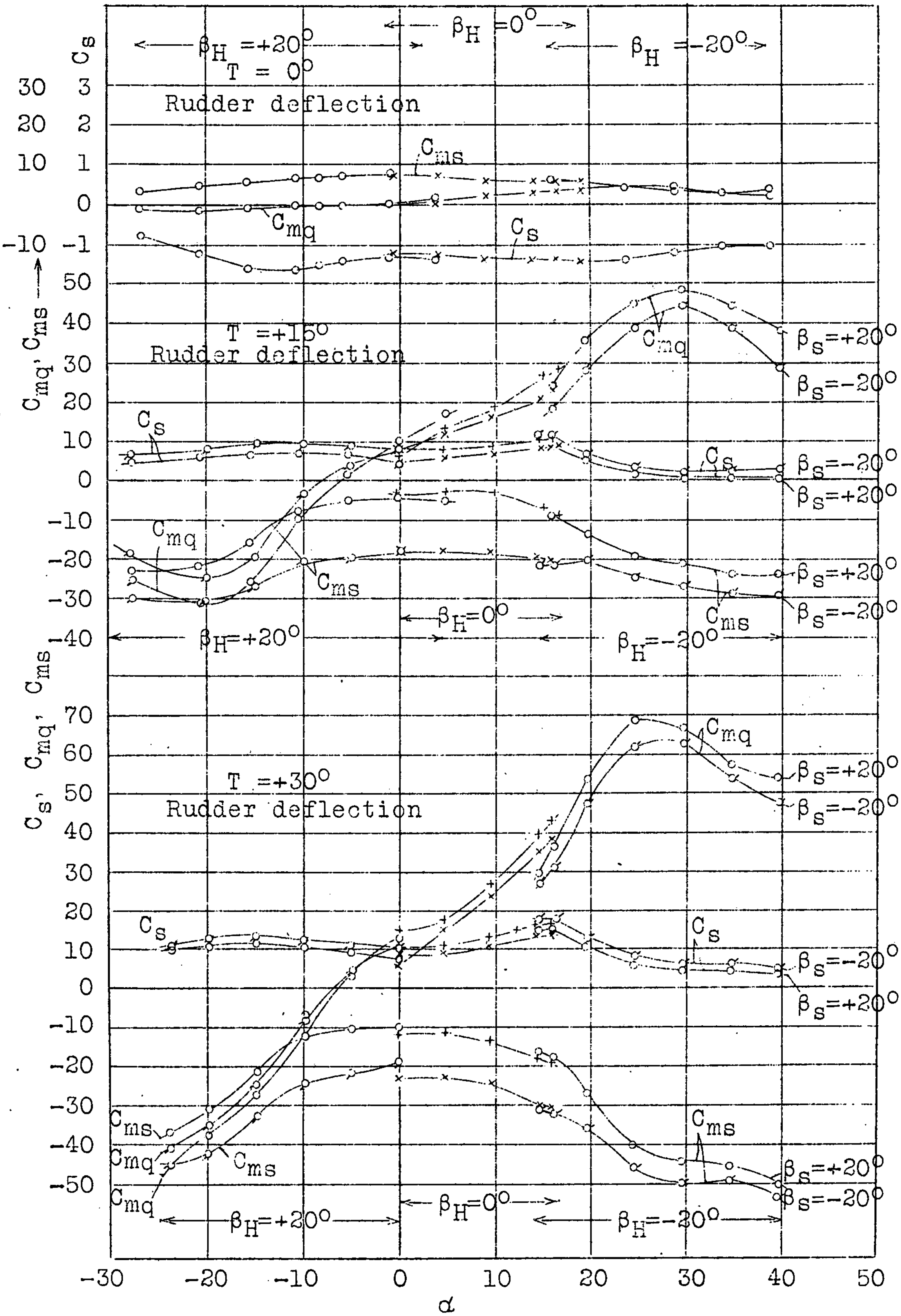

(Continuation of Fig.13.)

b

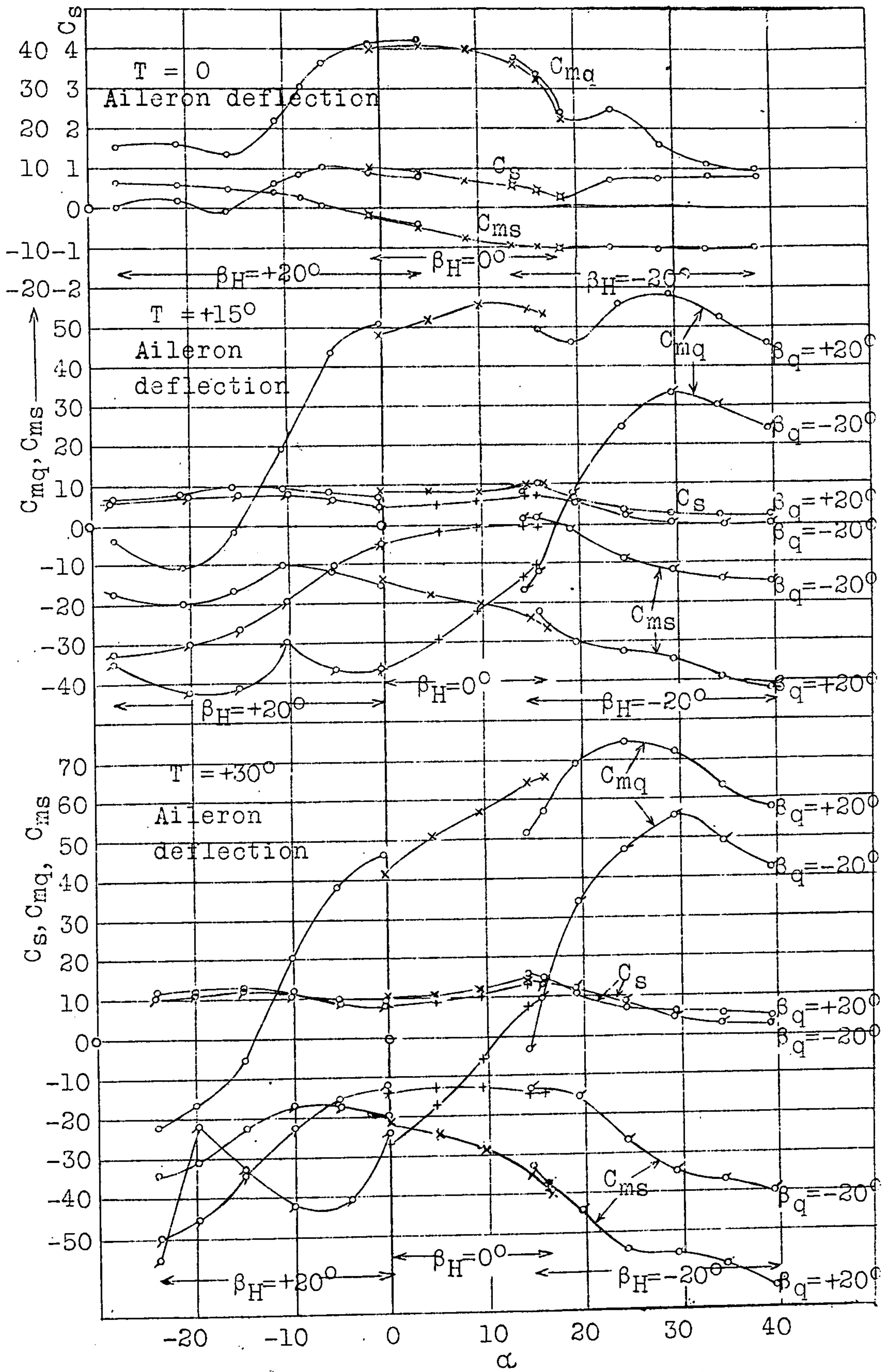

(Continuation of Fig.13.)

c

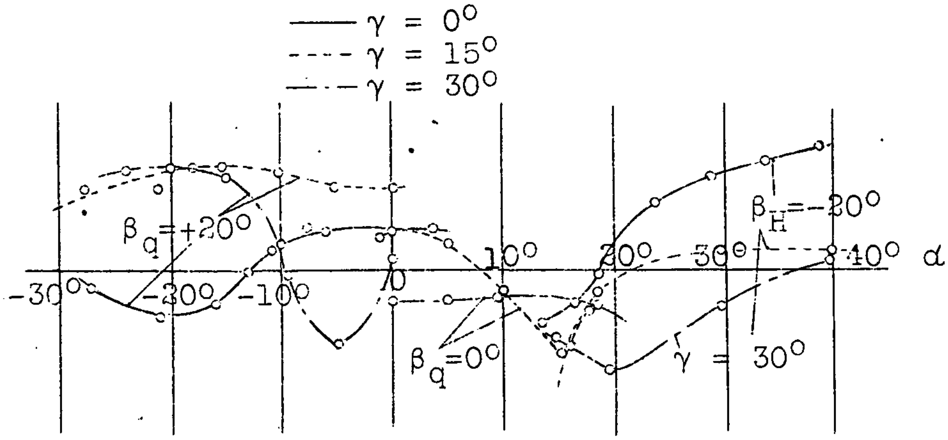

Fig.14 Effect of yaw on the pitching moments of U12. This is all the moment diagram which was determined. Unfortunately little use can be made of it because no measurement gave an elevator movement of zero.

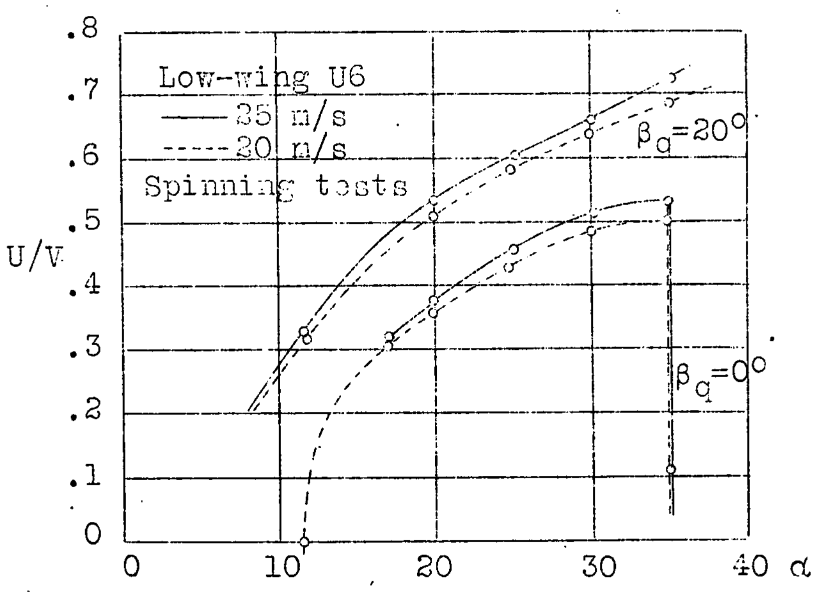

Fig.15 U6 spinning tests. A 20° aileron deflection gives considerably greater angular velocity than no deflection. With increasing wind velocity the rotational speed likewise increases. The same is also true of the U7 and U12.(see Figs.16 and 17.)

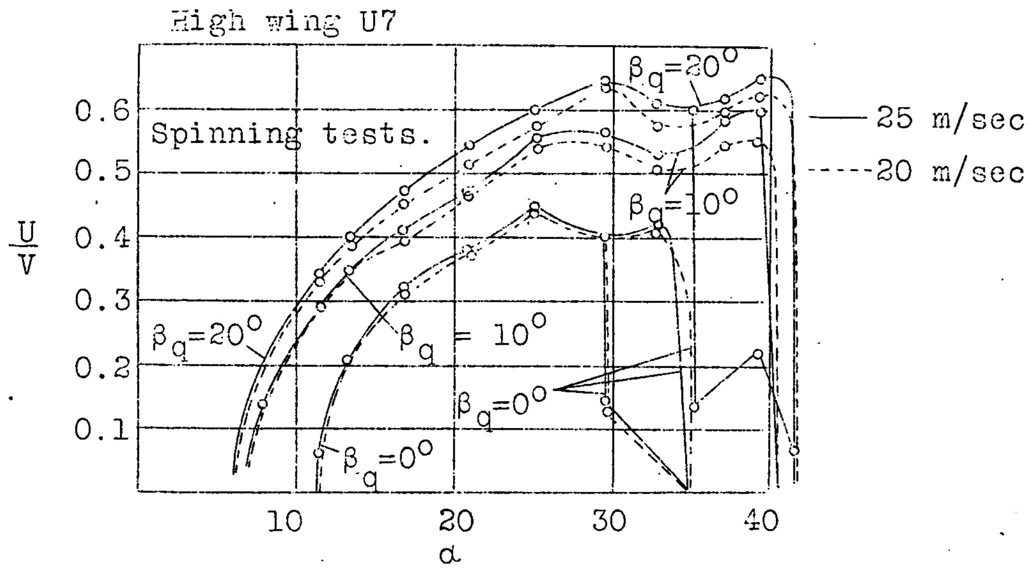

Fig.16 U7 Spinning tests. The aileron deflection and speed increase the angular velocity.

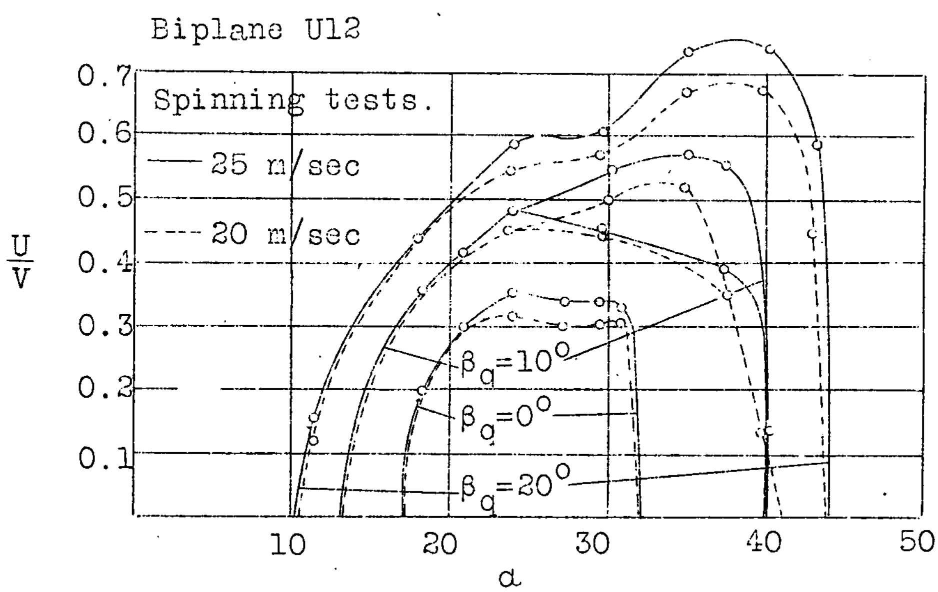

Fig.17 U12 Spinning tests. Here the angular velocity is a minimum for angular deflection, $\beta_q = 0$, and a maximum for $\beta_q = 20^\circ$. Their orders of magnitude agree fairly well with the flight-tests results. No accurate comparison is possible, because the magnitudes of the aileron deflections in the flight-test are lacking.

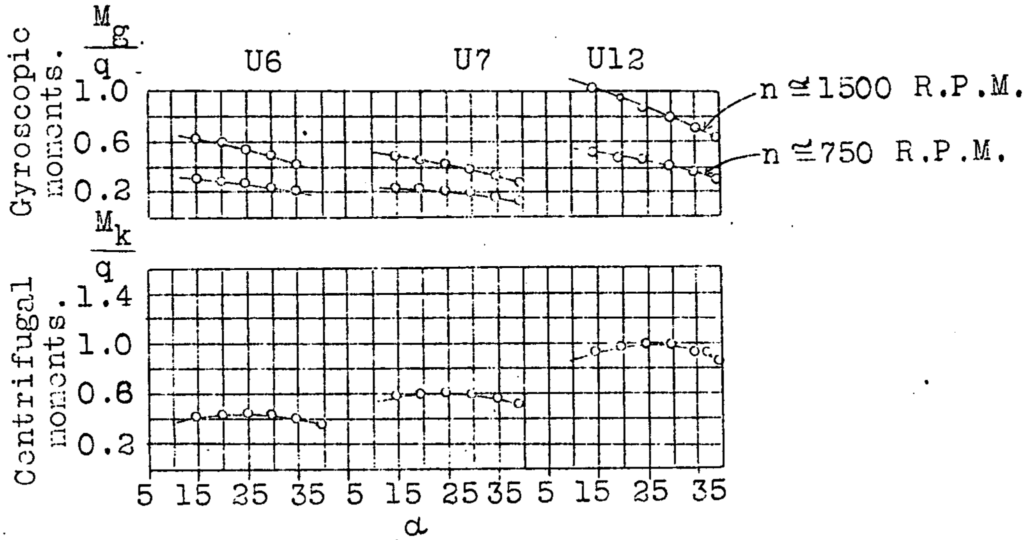

Fig.18 Inertia forces for an angular velocity ω=1. The centrifugal moment is least on the low wing monoplane. The Gyroscopic moments correspond to 750 and 1500 R.P.M. that is full throttle. One must never forget that the gyroscopic moments increase with the first power of the angular velocity and the centrifugal moments increase with the second power.

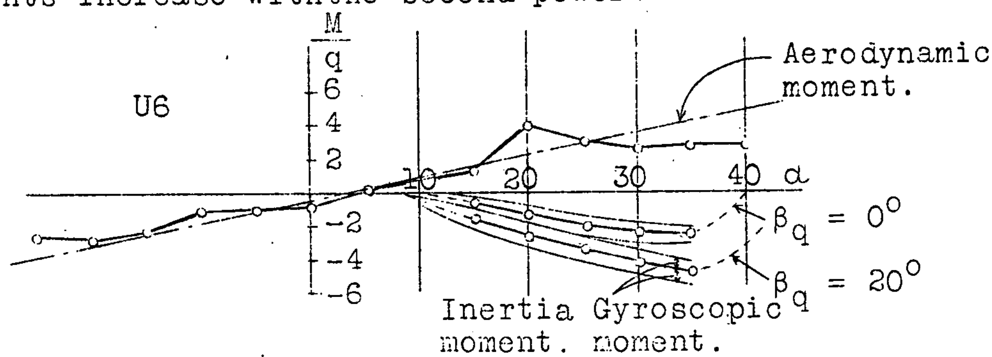

Fig.19 U6 Pitching moments and inertia forces. The upper line corresponds to the pitching moment in steady flight. The lower curves represent the inertia forces. The gyroscopic moments are introduced as thin lines for right and left spins. The insufficient excess of the air forces over the inertia forces is shown.

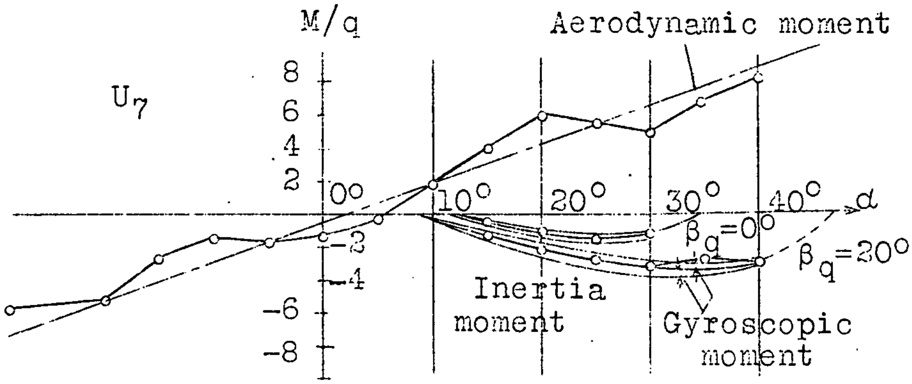

Fig.20 U7 Pitching moments and inertia forces. The aerodynamic pitching moment is almost twice as great as for the U6, which has almost the same wing and tail. On referring to Fig.18, it is seen that the square of the angular velocity is decisive. The effective inertia forces are therefore smaller than for the U6. The gyroscopic moments are again indicated as thin lines for right and left spins.

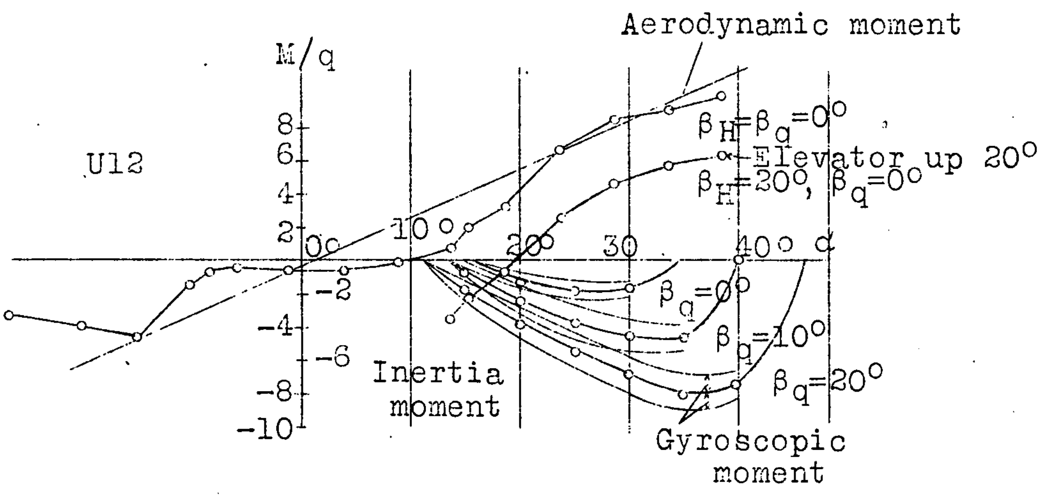

Fig.21 U12 Pitching moments and inertia forces. The magnitude of the aerodynamic pitching moment is conspicuous. The airplane was equipped and spun with a larger elevator than that used in the wind-tunnel tests. In practice therfore the pitching moment is still greater. The airplane should recover immediately with the controls neutral and with some pressure.